UDC 624.014.2:614.84:519.2
Original scientific paper
Received: 31.01.2002.

Safety of steel structures under the influence of fire loads

Ivica Boko, Vinko Jović and **Bernardin Peroš**
University of Split, Faculty of Civil Engineering, Matice hrvatske 15, HR-21000 Split, CROATIA
e-mail: Ivica.Boko@gradst.hr, Vinko.Jovic@gradst.hr, Bernardin.Peros@gradst.hr

SUMMARY

The paper presents an analysis of the influence of various types of actual fire loads upon a given industrial structure - a steel warehouse. Six different fire loads were simulated with different quantities of combustible material and by varying floor surfaces covered by combustible material.

Using a zone model, based on an approximate formulation, for different fire loads, obtained by varying the surface of ventilation openings, it was possible to obtain the temperature curves as a function of time which were used as the temperature load upon the supporting steel structure.

The model of transient non-linear heat transfer was used to analyse the influence of the shape of the cross-section of the steel structure in the case of standard fire. For specific cross-sections of a steel structure (non-protected and protected) the temperatures for six different cases of actual fires were determined.

***Key words**: actual fire load, transient non-linear heat transfer, temperature curves, section factor.*

1. INTRODUCTION

According to current scientific research findings in the field of fires, their breakout and growth (development/expansion), it is not possible to predict where and when a fire might break out. Fires in industrial objects can be caused by various factors, the most significant being man. Most fires are caused by men either directly (sabotage, bombing) or indirectly (malfunctions due to improper maintenance) and only a small part of fires is caused by natural disasters.

The products of a fire are: the development of high temperatures and great quantities of smoke in enclosures. High temperatures influence the supporting structure of the building, while smoke threatens humans, since most loss of life in fires is caused by smoke inhalation. This paper deals only with the effect of high temperatures upon the supporting steel structure.

During the last few years significant efforts have been made in scientific research to understand the process of the breakout of fires and their growth so that there is a specific scientific discipline referred to as “Fire Science”. Immediately after ignition a fire displays characteristics of a fire in open space. During the expansion period, the average temperature in the enclosure is low and the fire is localized. The heat released by gases heats the material which has not yet burst into flames. The transition from the fire breakout into a fully developed fire occurs as soon as the flames reach the ceiling and expand along it. Then high temperatures develop which can cause the collapse of the supporting structure. That phase is followed by the combustion phase which is characterised by a decrease in temperature of the enclosure. Fire in industrial buildings passes through all these phases unless the fire expansion has been prevented by various means (sprinklers, fire brigades).

During the last few years various numerical models have been developed in order to simulate these phases of a fire so that the obtained results are compared with actual fires or experimental fires.

2. MAIN CHARACTERISTICS OF FIRES IN THE ENCLOSURES

It has already been mentioned in the introduction that fire in enclosures, e.g. industrial buildings, passes through certain phases, as presented in Figure 1.

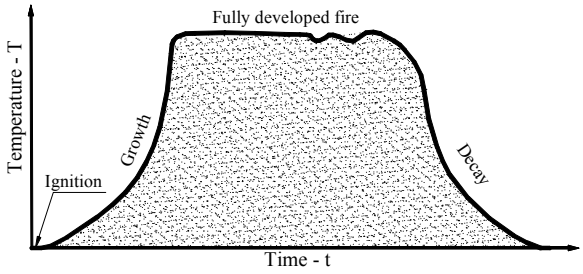

Fig. 1 Growth phase of fire

Immediately after ignition, the fire exhibits the characteristics of fires in open spaces. During the fire growth phase the average temperature of the enclosure is low and the fire has the characteristics of a localised fire. The fire develops by flames spreading along the burning surfaces or surrounding objects. This phase is characterised by the appearance of smoke and flames which increase the temperature of the enclosure. The fire growth phase lasts ca *10-20 minutes*, i.e. until the flames reach the ceiling and run along its surface. The heat released by hot gases heats the materials which have not yet been engulfed by flames. The next phase is fully developed fire in which the highest temperature is reached. It has been proved by experiments [1] that this phase is critical and if it continues to develop the burning rate of the fuel is increased. This increase in the burning rate, for the vertical increase of a flame height of *1 meter*, results in an increase in the horizontal flame expansion from *5* to *7 meters*. These ceiling flames dramatically increase the level of radiation falling on unburnt fuel remote from the origin of the fire. This alone can result in a rapid increase of the fire spread irrespective of other factors. Once this occurs, a relatively small fire rapidly becomes large.

After reaching the phase of the fully developed fire (i.e. the maximum burning rate), experiments have shown that the fire action is defined by two factors: the quantity and nature of the fire load and the supply of oxygen (air) for combustion.

In enclosed spaces with a volume less than *100* m^3 the phase of fully developed fire is proceeded by a flashover. Due to an increased quantity of smoke gases and radiation from flames the ambient temperature is increased and when the temperature increases to ca *600° C*, in the layer below the ceiling, the flames spread along the surface of the combustibles. This process of flames spreading lasts a short time and looks spectacular. This transitory phase leading to a fully developed fire is generally analyzed separately.

Finally, when the ambient temperature in the enclosed space falls to *80%* of the maximum temperature, the last phase, the combustions phase, can be observed.

The most important factor for a fire is the fuel/ combustible material. In order to analyze fires it is necessary to know the nature and quantity of the fuel, its burning rate as well as the fire intensity and its duration.

The most relevant property of each fire load is the burning rate, i.e. the quantity of the heat released per unit floor area of the fire load, expressed as wood equivalent. In cases of actual fires it is difficult to estimate the burning rate but it can be derived if the quantity of fuel present before the fire and that remaining after extinction, can be determined along with the duration of the fire.

The burning rate per unit of the affected floor area can be expressed by two characteristic quantities:

- ratio between the burnt material expressed as the wood equivalent and the estimated area of the floor covered by the fire load in the fire zone and fire duration,
- ratio between the total quantity of the fire load expressed as wood equivalent and the estimated floor surface covered by combustible material multiplied by the load density.

The first two quantities are used to express the global burning rate per unit of floor area covered by the fire load, while the second quantity is used to define the velocity of the mass losses, which define the burning rate. The burning rate decreases with an increase in the fuel density and is better correlated than the burning rate expressed by the fire load per unit of floor area covered by that load. The fire load density is very significant for determining the fire characteristics. Both ratios for representing the burning rate are better that those associated with the ratios of whole combustibles, expressed as wood equivalent, per unit floor area of the enclosure.

The regression equation for the determination of the maximum burning rate is:

$$\dot{m}'' = 0.11\,\rho^{-0.34} \tag{1}$$

with the correlation coefficient *0.61*, where $\dot{m}''$ is the maximum burning rate per unit of fire floor area, and ρ is the fuel density (mass per unit of fuel height and the floor area covered by the fire load).

The variation coefficient for determining the burning rate is *0.7*.

The fire duration is the same as the duration of a fully developed fire. In this case, as well as when determining the burning rate, there are several factors to be used for defining the fire duration. The most important three factors are:

- ratio between the fuel, expressed as wood equivalent, and the total area of the enclosure,
- ratio between the fuel, expressed as wood equivalent per unit of area covered by fuel,
- fuel height.

The regression analysis, according to data obtained both from experimental and actual fires, yields two equations [1]:

$$t = 590 \cdot f^{0.30} \; sec \tag{2}$$

where *f* is the fuel mass, expressed as wood equivalent per unit of floor area of the enclosure with a correlation coefficient of *0.62*, and:

$$t = 126 \cdot f^{0.48} \; sec \tag{3}$$

where *f* is the fuel mass (load) expressed as wood equivalent per unit of floor area covered by fuel with a correlation coefficient of *0.70*. In order to achieve better correlation the second equation, which depends upon the floor area covered with fuel, has been chosen as the equation for determining the fire duration. Fire intensity can be expressed depending upon the burning rate and fire duration. Fire intensity can be defined as a quantity of heat released in a time unit during the fire incident.

Fire modelling necessitates knowing the fire curve, i.e. the fire intensity- time curve. As previously noted, fire passes through three phases:

- growth phase,
- fully developed fire phase - constant phase,
- decay phase.

The fire growth phase can be defined by the expression:

$$\dot{Q} = \alpha_r \cdot t^2 \tag{4}$$

where $\dot{Q}$ is the heat release rate *[kW]*, α_r is fire growth factor *[kW/s²]*, and *t* is time *[sec]*.

The fire growth factor is determined experimentally. The conceptual probability density distribution of the fire growth factor is presented in Figure 2.

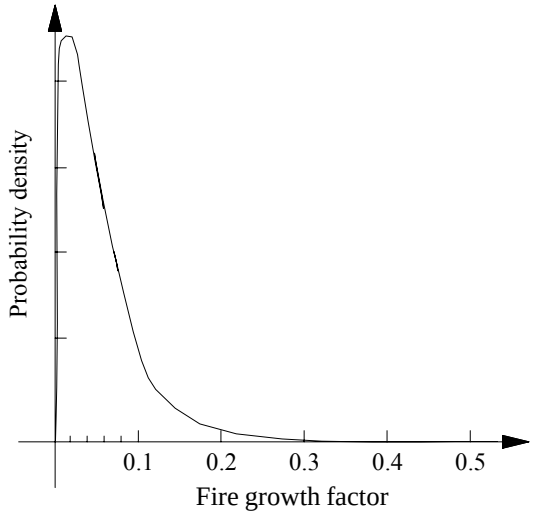

Fig. 2 Conceptual probability density distribution α_r

The development phase is followed by the fully developed fire phase. In modelling this phase the maximum fire intensity is considered as constant in time. In this phase the highest temperatures in the enclosure are developed and they represent the most critical phase of the fire. This phase, in which *70%* of the fuel is burnt, is followed by the decay phase when the temperatures in the enclosure are decreased. It is assumed that in this phase the fire intensity decreases linearly with time and that the total fuel mass is burnt.

The model of the heat release rate - time curve is presented in Figure 3.

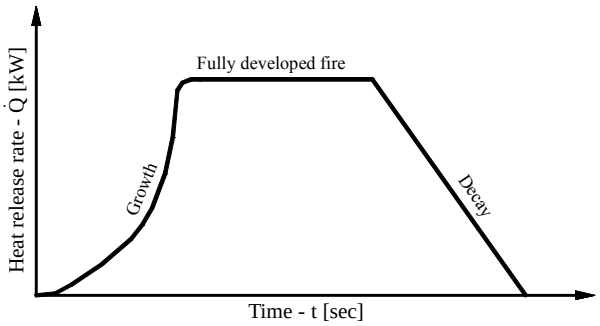

Fig. 3 Heat release rate - time curve

3. COMPUTATION OF TEMPERATURES IN ENCLOSURES

The starting assumption for the computation of temperatures caused by the fire action in an enclosure is that the enclosure can be divided into a certain number of zones so that each zone has approximately the same physical characteristics (mass, density, temperature, pressure and internal energy) since the real simulation is a very complex task in numerical modelling so that certain simplifications are introduced.

Fire modelling in zones starts with the system of differential equations which are derived by using the mass conservation law (continuity equation), energy maintenance law (first law of thermodynamics) and the law of ideal gases. These laws are put forward for each zone. Most frequently the enclosure is divided into two zones: the upper zone - the zone of hot gases and the lower zone - the zone in which the ambient temperature and pressure are retained.

The interaction between the zones is the consequence of the exchange between mass and energy. The following simplifications are introduced into such modelling:

- specific heats c_p and c_v are taken as constant,
- hydrostatic conditions have been neglected - the law of ideal gases.

Fire modelling in zones can be generally described by two formulations: conservative and approximate; the latter formulation has been used in the paper.

Approximate formulations assume that the pressure in the enclosure and the temperature in the lower zone remain ambient. With these two assumptions, unlike the conservative formulation, it is possible to get a system of two differential equations with two unknowns [2]:

- differential equation of the mass conservation law in the upper zone:

$$\frac{dm}{dt} = \sum \dot{m}_i \tag{5}$$

- differential equation for the upper zone energy (by using the law of ideal gases):

$$\frac{dy}{dt} = -\frac{\sum \dot{q}_i}{Ac_p \rho_\infty T_\infty} \tag{6}$$

where $\dot{m}_i$ is the measure of mass inflow (change of mass in time), t is time, y is the height of the bottom of the upper zone surface, q_i is the enthalpy of the upper zone, A is the enclosure surface, c_p is specific heat at constant pressure, ρ_∞ is air density at room temperature, and T_∞ is room temperature.

4. NUMERICAL EXAMPLES FOR THE DETERMINATION OF TEMPERATURES IN ENCLOSURES

In order to determine critical temperatures in large buildings the JET program [2] was used to simulate a fire in a closed industrial warehouse. The dimensions of the considered warehouse were *60x40 m*. The lowest height of the supporting structure was *7.5 m*. The fuel considered in this case was wood, used in experimental investigations [1]. The paper presents six examples of actual fire loads by varying the following parameters:

- fuel mass per unit area,
- floor surface covered by fuel.

The fuel mass per unit area varied according to the following values:

- *35 kg/m²* (filled mail bags *1.9 m* high)
- *70 kg/m²* (PE shower cabins packed in cardboard boxes *2.5 m* high)
- *105 kg/m²* (PE bottles in cardboard boxes *2.2 m* high),

The floor surface covered by fuel varied according to the following values:

- *5%* of the total structure area,
- *10%* of the total structure area.

The surface of openings varied according to the following values:

- *1.0%* of the roof and wall surfaces,
- *2.0%* of the roof and wall surfaces,
- *5.0%* of the roof and wall surfaces,
- *10.0%* of the roof and wall surfaces.

In Example 1 a fuel mass of *35 kg/m²* and *5%* of the total surface of the structure were covered by fuel, in Example 2 the considered fuel mass was *70 kg/m²* and *5%* of the surfaces covered by fuel, in Example 3 the considered fuel mass was *105 kg/m²* with *5%* of the surfaces covered by fuel, in Example 4 the fuel mass was *35 kg/m²* and *10%* of the surfaces covered by fuel, in Example 5 the fuel mass considered was *70 kg/m²* and *10%* of the surfaces covered by fuel, and in Example 6 the fuel mass was *105 kg/m²* and *10%* of the structure surfaces was covered by fuel. The obtained results, for the least favourable case of ventilation of *1%*, depending upon the radial distance from the fire source *r*, are presented in Figures 4 and 5.

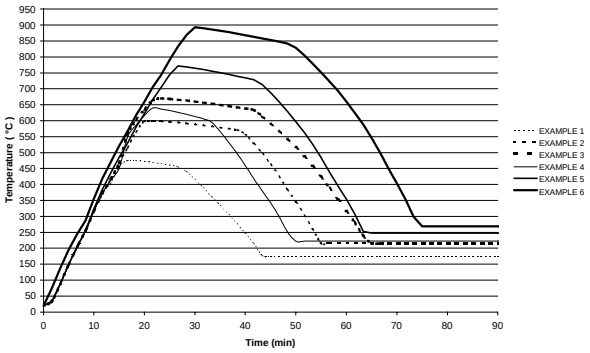

Fig. 4 Ceiling temperature curve for r=0.0 m

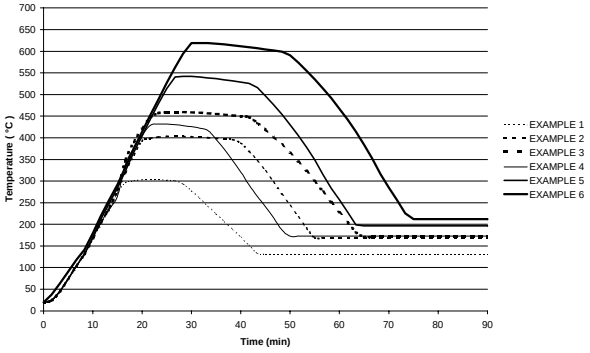

Fig. 5 Ceiling temperature curve for r=7.0 m

5. MODELLING A TRANSIENT NON-LINEAR HEAT FLOW

A body with non-uniform temperatures attempts to make them uniform by a heat flow. All the points of the body with an equal instant temperature lie along the level-surface of equal temperatures. These surfaces can be placed in different ways, but they cannot be in contact or intersect, since it would imply the simultaneous occurrence of different temperatures, which is nonsense from the physical standpoint.

Heat flows in the direction of decreases in temperature, i.e. with greatest intensity in the direction of the normal to the level surface. Fourier's differential equation of heat flow in an isothropic body is:

$$\frac{\partial e}{\partial t} + \left(\frac{\partial q_x}{\partial x} + \frac{\partial q_y}{\partial y} + \frac{\partial q_z}{\partial z} \right) = Q \tag{7}$$

i.e.:

$$\dot{e} + \nabla \boldsymbol{q} = Q \tag{8}$$

$$\dot{e} = \frac{\partial e}{\partial t} = c\rho \frac{\partial T}{\partial t} \tag{9}$$

where e is the specific volumetric enthalpy, c is a specific heat capacity *[J/kgK]*, ρ is the density, T is the temperature *[°C]*, and Q is internally generated heat *[W/m^3]*.

The vector $\boldsymbol{q}$ of the heat flow along the coordinate axes can be given by the following expression:

$$\boldsymbol{q} = \begin{Bmatrix} q_x \\ q_y \\ q_z \end{Bmatrix} = -\boldsymbol{K} \begin{Bmatrix} \frac{\partial T}{\partial x} \\ \frac{\partial T}{\partial y} \\ \frac{\partial T}{\partial z} \end{Bmatrix} = -\boldsymbol{K}\ \nabla T \tag{10}$$

For an isotropic material:

$$\boldsymbol{K} = k\,\boldsymbol{I} \tag{11}$$

where k is the coefficient of thermal conductivity *[W/mK]*, and $\boldsymbol{I}$ is the unit matrix.

By introducing Eq. (10) into Eq. (8) we get:

$$\dot{e} - \nabla^T \left(\boldsymbol{K} \nabla T\right) - Q = 0 \tag{12}$$

In some materials the specific volumetric enthalpy is changed suddenly due to the changes of the phases at different temperatures, so that the specific volumetric enthalpy can be defined by the expression:

$$e(T) = \int_{T_0}^{T} \rho c\ dT + \sum_i \mathrm{l}_i \tag{13}$$

where l_i is the latent volumetric temperature caused by changes of phases in various temperature levels (e.g. due to water evaporation from the material).

Figure 6 presents a specific volumetric enthalpy dependent upon the temperature for the material with the latent volumetric temperature with the designated step l on the curve.

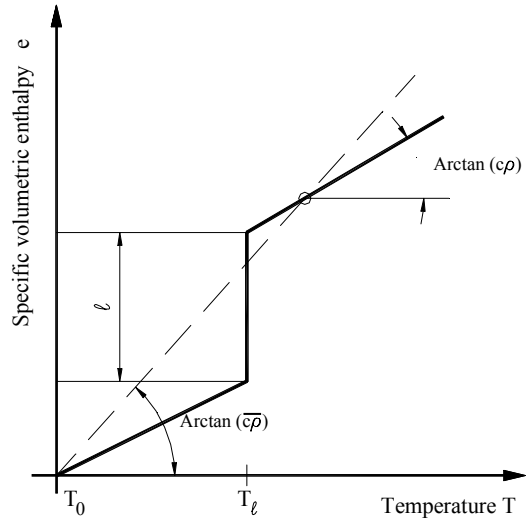

Fig. 6 Definition of the nominal specific volumetric enthalpy

It can be noted that at temperature T_l, where the enthalpy curve leaps, the value $c\rho$ is not defined, while the value $\overline{c\rho}$ is always defined, i.e. final.

The nominal specific volumetric enthalpy can be expressed according to:

$$e = \overline{c\rho}\ T \tag{14}$$

By introducing Eq. (14) into Eq. (12) we have:

$$\frac{\partial}{\partial t}\left(\overline{c\rho}\ T\right) - \nabla^T \left(\boldsymbol{K} \nabla T\right) - Q = 0 \tag{15}$$

Equation (15) presents the heat flow dependent upon time and space. In order to solve this equation it is necessary to know the initial and boundary conditions. Initial conditions have to define the temperature distribution in all points of the controlled volume in a known instant of time, generally at instant *t=0*. At the boundary of the controlled volume it is necessary to substitute the connection with the discarded section of the continuum, which is not modelled, i.e. with boundary conditions. A natural boundary condition is the heat flow along the continuum boundary, while the obligatory boundary condition is the given node temperature.

By applying the basic lemma [3] on Eq. (15) we have:

$$\int_{\Omega} w \left[\frac{\partial}{\partial t}\left(\overline{c\rho} T\right) - \nabla^T \boldsymbol{K}\ \nabla T - Q \right] d\Omega = 0 \tag{16}$$

and by applying the rule of partial integration, a weak formulation of heat flow is obtained:

$$\begin{aligned} &\int_{\Omega} w \frac{\partial}{\partial t}\left(\overline{c\rho} T\right) d\Omega + \int_{\Omega} \left(\nabla w\right)^T k \nabla T\, d\Omega = \\ &= \int_{\Gamma} w \vec{n}^T \boldsymbol{K} \nabla T\, d\Gamma + \int_{\Omega} wQ\, d\Omega \end{aligned} \tag{17}$$

where $\vec{n}$ is external normal upon the boundary Γ.

By choosing the test vector from the class of solutions variations, the boundary integral should be calculated only along the boundary sections with natural boundary conditions. A natural boundary condition is generally a function of the point position on the boundary and the solution:

$$q(x) = q_0 + \alpha_1 T + \alpha_2 T^2 + \ldots \quad ; x \in \Gamma \tag{18}$$

which can be formally developed into an order of power along variable T.

The heat flow along the continuum boundaries, which is caused by the difference between the continuum temperature and the ambient air, consists of two parts: the heat flow due to convection and the heat flow caused by radiation.

This phenomenon is too complex for a model, so that the model uses approximate formalae. The heat flow caused by convection is defined by the expression:

$$q_n^k = \beta\left(T_p - T_{pe}\right)^\gamma \tag{19}$$

and the heat flow resulting from radiation:

$$q_n^z = \varepsilon_r \sigma\left(T_p^4 - T_{pe}^4\right) \tag{20}$$

where β is the coefficient of heat transfer by convection *[W/m²K]*, T_p is the gas temperature surrounding the element (*K*), T_{pe} is the temperature of the element surface (*K*), γ is convection coefficient, ε_r is the resultant emission coefficient, and σ is Stefan-Boltzman's constant $5.667 \cdot 10^{-8}$ *[W/m²K⁴]*.

The resultant emission coefficient depends upon the surface characteristics and the geometry configuration. If the considered surface is relatively small with respect to the surroundings with the uniform heat distribution, the resultant emission coefficient is equal to the emission surface coefficient ε_{pe}. In cases of fire action upon a structure, the resultant emission coefficient is computed from the conditions of two infinitely large parallel planes, as follows:

$$\varepsilon_r = \frac{1}{\frac{1}{\varepsilon_{pe}} + \frac{1}{\varepsilon_p} - 1} \tag{21}$$

where ε_p is the emission coefficient for the respective gas or emission flame coefficient.

The total heat flow along the continuum boundaries is computed by adding the contibution of convection and radiation:

$$q_n = q_n^k + q_n^z \tag{22}$$

The finite element method uses localised global shape functions which are derived from the shape element functions. The shape functions are chosen so that the parameters of the linear combination are equal to the node values of an approximate solution:

$$T = \sum_i N_i(x, y, z) T_i(t) = \boldsymbol{N}\, \boldsymbol{T} \tag{23}$$

Since it is a transient problem the nodal values of the approximate solution are the time functions so that the change of temperature in time is:

$$\dot{T} = \boldsymbol{N}\, \dot{\boldsymbol{T}} \tag{24}$$

By choosing the test function as a variation of approximate solution (Gallerkin's method):

$$w_i = N_i \tag{25}$$

a system of non-linear differential equations is obtained:

$$\frac{\partial}{\partial t}\left[\int_\Omega \left(\boldsymbol{N}^T \overline{c\rho}\, \boldsymbol{N}\, d\Omega\right)\boldsymbol{T}\right] + \int_\Omega \left[(\nabla \boldsymbol{N})^T \boldsymbol{K}\, \nabla \boldsymbol{N}\, d\Omega\right]\boldsymbol{T} = \int_\Gamma \boldsymbol{N}^T \vec{n}^T \boldsymbol{K} \nabla \boldsymbol{T}\, d\Gamma + \int_\Omega \boldsymbol{N}^T Q\, d\Omega \tag{26}$$

Since the finite element method is based upon the localisation of the global base, the solution is expressed as a vector whose components are associated with the discretization nodes. Equation (26) can be expressed in a vector form:

$$\frac{\partial}{\partial t}(\boldsymbol{e}) + \boldsymbol{f}_T = \boldsymbol{f}_q + \boldsymbol{f}_Q \tag{27}$$

where:

- $\boldsymbol{e}$ - enthalpy vector or heat accumulated in the element associated to neighbouring nodes,
- $\boldsymbol{f}_T$ - vector of the nodal heat flow,
- $\boldsymbol{f}_q$ - vector of the boundary heat flow,
- $\boldsymbol{f}_Q$ - vector of heat load.

The components of vectors $\boldsymbol{e}$, $\boldsymbol{f}_T$ and $\boldsymbol{f}_Q$ are associated with the domain nodes, while the components of vector $\boldsymbol{f}q$ are associated with the boundary nodes.

The vector of nodal enthalpy is:

$$\boldsymbol{e} = \boldsymbol{C}\, \boldsymbol{T} \tag{28}$$

where $\boldsymbol{C}$ is nominal thermal capacity matrix.

The vector of internal heat transfer is:

$$\boldsymbol{f}_T = \boldsymbol{K}\, \boldsymbol{T} \tag{29}$$

where $\boldsymbol{K}$ is transfer matrix.

By introducing Eqs. (28) and (29) into Eq. (27) a discrete system of equations is obtained:

$$\frac{\partial}{\partial t}(\boldsymbol{C}\, \boldsymbol{T}) + \boldsymbol{K}\, \boldsymbol{T} = \boldsymbol{f}_q + \boldsymbol{f}_Q \tag{30}$$

Equation (30) can be presented as dependent upon nodal enthalpy:

$$\frac{\partial}{\partial t}(\boldsymbol{e}) + \boldsymbol{K}^*\, \boldsymbol{e} = \boldsymbol{f}_q + \boldsymbol{f}_Q \tag{31}$$

where:

$$\boldsymbol{K}^* = \boldsymbol{K}\, \boldsymbol{C}^{-1} \tag{32}$$

In the same way, Eq. (30) can be written also for each finite element, as a separate whole, with its local boundary conditions:

$$\frac{\partial}{\partial t}\left(\boldsymbol{C}^e\, \boldsymbol{T}\right) + \boldsymbol{K}^e\, \boldsymbol{T} = \boldsymbol{f}_q^e + \boldsymbol{f}_Q^e \tag{33}$$

i.e. expressed by nodal enthalpy:

$$\frac{\partial}{\partial t}(\boldsymbol{e})^e + \left(\boldsymbol{K}^*\, \boldsymbol{e}\right)^e = \boldsymbol{f}_q^e + \boldsymbol{f}_Q^e \tag{34}$$

The elements of matrices and vectors of a finite element in Eq. (33) are:

$$\boldsymbol{K}_{ij}^e = \int_e (\nabla N_i)^T\, \boldsymbol{K}\left(\nabla N_j\right) de \tag{35}$$

$$\boldsymbol{C}_{ij}^e = \int_e N_i\, \overline{c\rho}\, N_j\, de \tag{36}$$

$$\boldsymbol{f}_{qi}^e = \int_\gamma N_i\, \vec{n}^T\, \boldsymbol{K} \nabla \boldsymbol{T}\, d\gamma \tag{37}$$

$$\boldsymbol{f}_{Qi}^e = \int_e N_i\, Q\, de \tag{38}$$

The values of the integral in Eqs. (35) to (38) are computed by using Gauss's square formula.

The term transient process implies a phenomenon which is changeable in time. Such a phenomenon is observed from a known state, i.e. from initial conditions.

The finite element method leads to a discrete system of ordinary non-linear differential equations:

$$\frac{d}{d\,t}(\boldsymbol{e}) = -\boldsymbol{K}^{*}\,\boldsymbol{e} + \boldsymbol{f} \tag{39}$$

where:

$$\boldsymbol{f} = \boldsymbol{f}_q + \boldsymbol{f}_Q \tag{40}$$

By applying an approximate form of the theorem about the mean value [3] to Eq. (39) the following expression is obtained:

$$\begin{aligned}&\theta\,\boldsymbol{K}^{*}_{t+\Delta t}\,\boldsymbol{e}_{t+\Delta t} + (1-\theta)\boldsymbol{K}^{*}_{t}\,\boldsymbol{e}_{t} + \frac{\boldsymbol{e}_{t+\Delta t} - \boldsymbol{e}_{t}}{\Delta t} = \\ &= \theta\,\boldsymbol{f}_{t+\Delta t} + (1-\theta)\,\boldsymbol{f}_{t}\end{aligned} \tag{41}$$

where:

t - beginning of the time interval,
$t+\Delta t$ - end of the time interval,
θ - interpolation parameter.

By the selection of sufficiently close time intervals it can be assumed that the subintegral function is monotonous in a more general sense within the time interval Δt, so that the value of the interpolation parameter ranges from $0<\theta<1$.

When $\theta=0$, the method for computing the unknowns at the time of the time interval becomes explicit, i.e. determined by the known values, indirectly. Such a selection corresponds to Euller's explicit method. By choosing the values $\theta=1$, the unknown value at the end of the time interval can be determined implicitly, so that a system of equations has to be solved in order to determine the value of the new state. When the values of the interpolation parameter are $0<\theta<1$, it is a combined method. For the value $\theta=0.5$ it is the method of central differences which is a method of the second order approximation. For the linear problems, $\theta\geq 0.5$ when the method will be unconditionally stable, i.e. for any time increment Δt the method always converges. The explicit method will converge only if the time increment Δt is smaller than the critical t_{cr}. The value of the critical time increment depends upon the element size, the material properties and boundary conditions.

For $\theta=0$ in Eq. (41) the explicit formula is:

$$\boldsymbol{e}_{t+\Delta t} = \boldsymbol{e}_{t} + \left(\boldsymbol{f}_{t} - \boldsymbol{K}^{*}_{t}\,\boldsymbol{e}_{t}\right)\Delta t \tag{42}$$

Equation (28) is then used to obtain temperature at a node i:

$$T_{i,t+\Delta t} = C_{ii}^{-1}\left(T_{i,t+\Delta t}\right)E_{i,t+\Delta t} \tag{43}$$

If C_{ii} varies with temperature the exact solution of Eq. (43) is obtained by iteration. However, if all elements around a node i are of the same material the specific volumetric entalphy is calculated as:

$$e_{i,t+\Delta t} = \frac{E_{i,t+\Delta t}}{W_{ii}} \tag{44}$$

and $T_{i,t+\Delta t}$ is obtained by using the temperature - specific volumetric entalphy relation as shown in Figure 7.

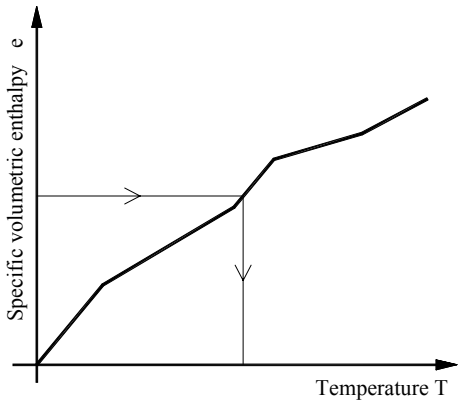

Fig. 7 Translation of specific volumetric enthalpy into temperature

For nodes at interfaces between elements of different materials, the following iteration formula is used to calculate temperature:

$$T^{j+1}_{i,t+\Delta t} = C_{ii}^{-1}\left(T^{j}_{i,t+\Delta t}\right)E_{i,t+\Delta t} \tag{45}$$

where j refers to iteration steps. For the first iteration step temperature from the previus time step is assumed. Iteration terminates when the difference between the nodal temperature from two successive iterations is less than a permisible value δ expressed as:

$$\frac{T^{j+1}_{i,t+\Delta t} - T^{j}_{i,t+\Delta t}}{T^{j+1}_{i,t+\Delta t} + T^{j}_{i,t+\Delta t}} < \frac{\delta}{2} \tag{46}$$

6. EXAMPLES OF TRANSIENT NON-LINEAR HEAT FLOW THROUGH THE BASIC MATERIAL OF THE STEEL STRUCTURE

In steel elements, the computation of temperatures caused by fires incidents was performed by applying the model of transient, non-linear heat flow and by using a program package TASEF [6]. TASEF (Temperature Analysis of Structures Exposed to Fire) is a computer program for the computation of temperatures exposed to fire based on the finite element method, for solving 2D problems.

For a standard fire [4] (standard temperature - time curve), by varying the factor of cross-sectional shape, an unprotected steel structure was analysed and the obtained results [7] are presented in Figure 8.

By varying fire loads, EXAMPLE 1 - EXAMPLE 6, for a given unprotected cross-section HEB 800 and a radial distance from the fire source *r=0.0 m* and *r=7.0 m*, the analysis was performed by using a transient, non-linear model, and the obtained results are presented in Figures 9 and 10.

Supporting steel structures can be protected by fire-resistant materials which will reduce the temperatures in case of fire incidents. One of the methods of protection is presented in Figure 11 where the steel structure was protected by incombustible mineral plates. The aim of this protection was to prevent the heating of the steel structure to critical temperature, which can result in the collapse of the structure.

The results obtained by the analysis of the protected cross-section are presented in Figure 12.

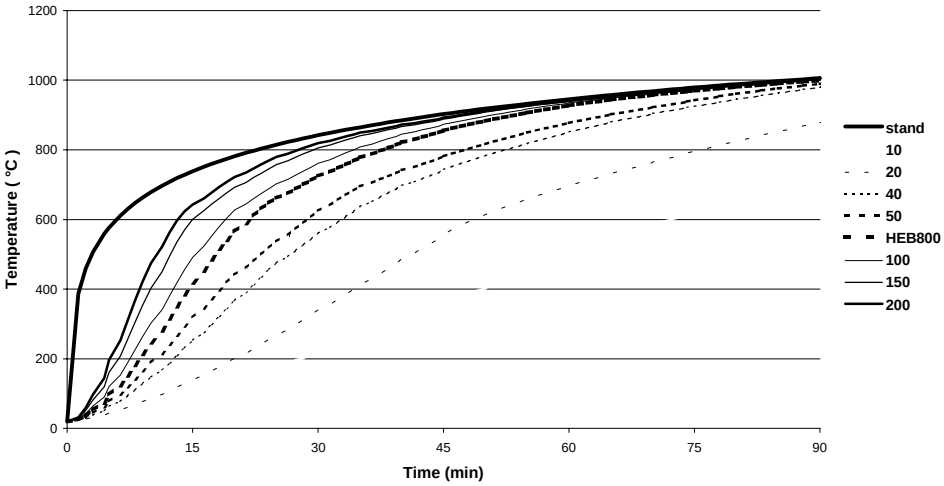

Fig. 8 Temperature-time curve for a standard fire depedent upon the section factor

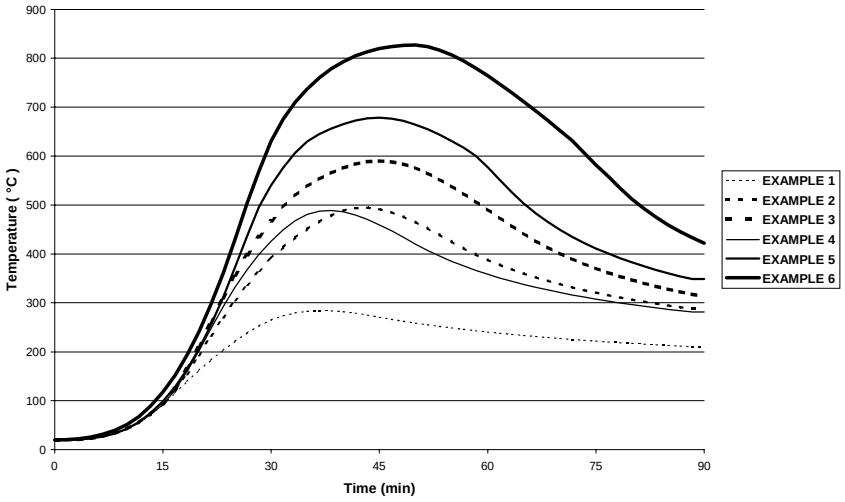

Fig. 9 Temperature - time curve r = 0.0 m

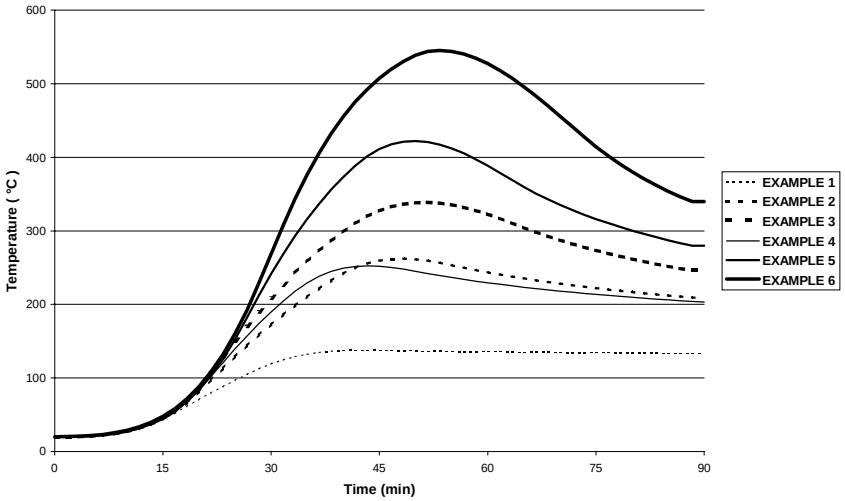

Fig. 10 Temperature - time curve r = 7.0 m

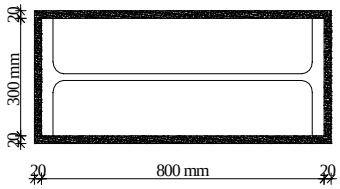

Fig. 11 Protection of the supporting steel structure by incombustible mineral plates

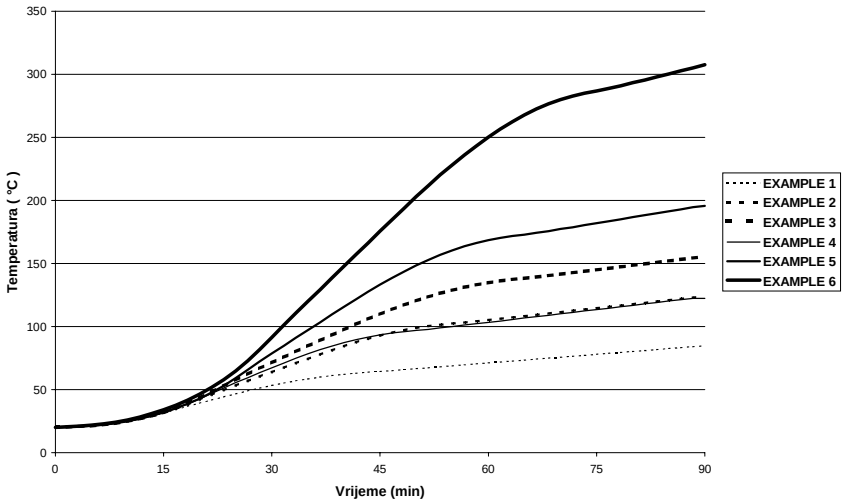

Fig. 12 Temperature - time curve r = 0.0 m

7. CONCLUSION

Fire action was simulated for a given steel structure with the dimensions *40×60×7.5 m* by applying the zone model, based on an approximate formulation. The results obtained by applying the zone model in six cases of fire load show that the temperature in the enclosed space depends mainly upon the fuel mass, the floor surface covered by fuel, the surface of the ventilation openings and the radial distance from the fire centre. By modelling a transient, non-linear heat flow, results were obtained which show that the temperature distribution along the cross-section depends both upon the actual fire action, radial distance from the fire centre and upon the factor of the shape of the cross-section; it has also been proved that the temperatures in the cross-section can be reduced by protecting the steel structure.

8. REFERENCES

[1] C.R. Theobald, Growth and development of fire in industrial buildings, *Fire Prevention and Technology*, pp. 4-16, 1977.

[2] W.D. Davis, *The Zone Fire Model JET: A Model for the Prediction of Detector Activation and Gas Temperature in the Presence of a Smoke Lay*er, NIST - National Institute of Standards and Tehnology, 1999.

[3] V. Jović, *Introduction to the Engineering Numerical Modelling*, Aquarius Engineering, Split, 1993. (in Croatian)

[4] Eurocode 1 - Basis of design and actions on structures - Part 2-2: Actions on structures - Action on structures exposed to fire, European Committee for Standardization, Brussels, 1995.

[5] Eurocode 3 - Design of steel structures - Part 1-2: General rules - Structural fire design, European Committee for Standardization, Brussels, 1995.

[6] E. Sterner and U. Wickstrõm, *TASEF - Temperature Analysis of Structures Exposed to Fire*, Swedish National Testing Institute, 1990.

[7] I. Boko, Safety of steel structures under the influence of fire loads, Master's Thesis, Faculty of Civil Engineering, University of Split, Split, 2001.

SIGURNOST ČELIČNIH KONSTRUKCIJA U SLUČAJU DJELOVANJA POŽARNOG OPTEREĆENJA

SAŽETAK

U radu je za odabrani industrijski objekt - skladišnu čeličnu halu, provedena analiza djelovanja različitih slučajeva realnog požara. Simulirano je 6 različitih požarnih opterećenja gdje se variralo količinom gorivog materijala i površinom poda objekta prekrivenog gorivim materijalom.

Primjenom modela zona, osnovanog na aproksimativnoj formulaciji, za različita požarna opterećenja, variranjem površine ventilacijskih otvora, dobivene su temperaturne krivulje u funkciji vremena, koje su korištene kao temperaturno djelovanje na nosivu čeličnu konstrukciju.

Modelom nestacionarnog nelinearnog provođenja topline analiziran je utjecaj faktora oblika poprečnog presjeka čelične konstrukcije u slučaju djelovanja standardnog požara. Za karakteristični poprečni presjek čelične konstrukcije (nezaštićena i zaštićena) određene su temperature u 6 različitih slučajeva realnog požara.

***Ključne riječi**: realno požarno opterećenje, nestacionarno nelinearno provođenje topline, temperaturne krivulje, faktor oblika presjeka.*